CSMA 2026
17ème Colloque National en Calcul des Structures
18-22 Mai 2026, Presqu'île de Giens (Var)

Two-Point Correlation Function Models for Polycrystals with Wide Grain Size Distributions

S. Khazaie[1], N. Sheng[1]

[1] *Nantes Université, École Centrale Nantes, CNRS, GeM, UMR 6183, F-44000 Nantes, France*
{shahram.khazaie@univ-nantes.fr, ningyue.sheng@ec-nantes.fr}

Abstract — Ultrasonic attenuation models for the characterization of polycrystalline materials rely on the two-point correlation function (TPCF). The classical exponential TPCF is insufficient for materials with wide grain size distributions (GSDs) commonly found in industrial polycrystals. This paper evaluates three different TPCF models that explicitly incorporate GSD statistics. We compare the models proposed by Argüelles and Turner, Sha, and a new model. The models are validated against TPCFs estimated from synthetic microstructures with varying GSD widths. Attenuation predictions are then compared to numerical data.
Keywords — Grain size distribution, Ultrasonic attenuation, Two-point correlation function.

1 Introduction

Ultrasonic techniques are among the primary methods used for the nondestructive evaluation (NDE) of polycrystalline materials [9, 8]. Theoretical frameworks developed by Stanke and Kino [10] and Weaver [12] model the scattering-induced attenuation of elastic waves, providing a link between measurable ultrasonic response and the material's microstructure. Central to these theories is the spatial two-point correlation function (TPCF), $\eta(r)$, which describes the probability that two points separated by a distance r reside within the same grain [11]. Historically, a simple exponential TPCF, $\eta(r) = \exp(-r/\bar{L})$, has been used, where $\bar{L}$ is the mean chord length. This model, however, is governed by a single parameter and cannot account for the significant grain size distributions observed in real materials, where the coefficient of variation (CV) of the grain diameter, δ_D, can range from 0.22 to 0.84. This limitation has driven the development of more sophisticated TPCF models that incorporate the probability density function (PDF) of grain sizes, $p_D(x)$ [1, 6, 7]. This paper provides a direct comparison of three such models and assesses their validity, particularly for polycrystals with broad grain size distributions (GSDs).

2 TPCF models incorporating the GSD

In this section, we introduce three models that incorporate the GSD into the TPCF. We assume a lognormal distribution for the volumetric grain diameter D, characterized by its mean $\bar{D}$ and CV δ_D:

$$p_D(x) = \frac{1}{x\sigma_D\sqrt{2\pi}} \exp\left(-\frac{\ln^2(x/\tilde{D})}{2\sigma_D^2}\right) \mathbb{1}_{R^+}(x), \tag{1}$$

where $\tilde{D} = \bar{D}/\sqrt{1+\delta_D^2}$ is the median of D, $\sigma_D^2 = \ln(1+\delta_D^2)$ is the variance of $\ln(D)$, which follows a Gaussian distribution denoted as $\mathcal{N}(\mu_D, \sigma_D^2)$, and $\mathbb{1}_S(x)$ is the indicator function defined over the set S. The grain volumes V, whose PDF is denoted as $p_V(x)$, also follow a lognormal distribution. In the next two sections, we present two recently introduced models [1, 6], both based on the seminal work of Stanke [11].

2.1 Model 1: Argüelles and Turner (AT)

According to Stanke, an exponential TPCF describes the correlation structure of a polycrystalline sample whenever the crossings obtained by drawing random lines within its microstructure with grain boundaries

follow a Poisson distribution. This case has been referred to as *Poisson statistics* in Table 1 of Stanke [11]. The exponential TPCF reads $\eta(r) = \exp(-2r/x)$, where x is the grain equivalent diameter. Argüelles and Turner [1] proposed a TPCF by treating x as a random variable, and weighting the exponential TPCF by the grain size PDF:

$$\eta_{\mathrm{AT}}(r) = \int_0^\infty p_D(x) \exp\left(-\frac{2r}{x}\right) \mathrm{d}x. \tag{2}$$

This model has a fundamental limitation. When the grains are slightly penetrating spheres of the same size d, and thus $p_D(x) = \delta(x-d)$, where δ denotes the delta distribution, Stanke derived the TPCF of the corresponding microstructure as (see Table 1 in [11]) the following piecewise function:

$$\eta(r,d) = \left(1 - \frac{3}{2}\frac{r}{d} + \frac{1}{2}\left(\frac{r}{d}\right)^3\right) \mathbb{1}_{[0,d]}(r). \tag{3}$$

However, inserting the particular case where $p_D(x) = \delta(x-d)$ into Eq. (2) yields $\eta(r) = \exp\left(-\frac{2r}{d}\right) = 1 - 2\frac{r}{d} + 2(\frac{r}{d})^2 - \frac{4}{3}(\frac{r}{d})^3 + O\left((\frac{r}{d})^4\right)$, which is not the same as Eq. (3). Therefore, the TPCF introduced in Eq. (2) cannot describe the microstructure of polycrystals containing spherical grains of the same size.

2.2 Model 2: Sha

To address the aforementioned issue with the model of Argüelles and Turner, Sha [6] extended the TPCF of uniformly-sized spherical grains (Eq. (3)) to the case of a polycrystal with a GSD, $p_D(x)$, as:

$$\eta_{\mathrm{Sha}}(r) = \int_r^\infty p_D(x) \left(1 - \frac{3}{2}\frac{r}{x} + \frac{1}{2}\left(\frac{r}{x}\right)^3\right) \mathrm{d}x. \tag{4}$$

This model, by construction, reduces to Eq. (3) when $p_D(x)$ is a delta function. When D follows a log-normal distribution, this TPCF can be written as:

$$\begin{aligned}\eta_{\mathrm{Sha}}(r) =& \frac{1}{2}\,\mathrm{erfc}\left(\frac{\ln(r/\tilde{D})}{\sqrt{2}\sigma_D}\right) - \frac{3}{4}\tilde{D}^{-1}\exp\left(\frac{\sigma_D^2}{2}\right)\mathrm{erfc}\left(\frac{\ln(r/\tilde{D}) + \sigma_D^2}{\sqrt{2}\sigma_D}\right) r \\ &+ \frac{1}{4}\tilde{D}^{-3}\exp\left(\frac{9\sigma_D^2}{2}\right)\mathrm{erfc}\left(\frac{\ln(r/\tilde{D}) + 3\sigma_D^2}{\sqrt{2}\sigma_D}\right) r^3,\end{aligned} \tag{5}$$

where $\mathrm{erfc}(x) = \frac{2}{\sqrt{\pi}}\int_x^\infty \exp(-t^2)\mathrm{d}t$ denotes the complementary error function.

2.3 Model 3: A new model (SK)

In this section, we introduce a third model based on the definition of the TPCF for statistically equiaxed polycrystals containing spherical grains [7]. Let $\eta(\mathbf{r} = \mathbf{x} - \mathbf{x}')$ denote the probability that two points $\mathbf{x}$ and $\mathbf{x}'$ randomly chosen within a sample lie in the same grain. The hypothesis of equal-sized grains implies that this function depends only on the lag distance $r = |\mathbf{r}|$. Based on the law of total probability, the latter reads:

$$\eta(r = \|\mathbf{x}' - \mathbf{x}\|) = \int_0^\infty \mathbb{P}\left(g(\mathbf{x}') = g(\mathbf{x}) \;\middle|\; V_{\mathbf{x}} \in [v, v+\mathrm{d}v]\right) p_{V_{\mathbf{x}}}(v)\,\mathrm{d}v, \tag{6}$$

wherein the function g links the position of points to the grain numbers, and $V_{\mathbf{x}} = |g(\mathbf{x})|$ specifies the volume of the grain corresponding to the point $\mathbf{x}$. It should be noted that the distribution of the random variable $V_{\mathbf{x}}$ is not the same as that of V. The first term of the integrand in Eq. (6) can be calculated using basic geometry. For a lognormal distribution, this results in the following TPCF [7]:

$$\begin{aligned}\eta(r) =& \frac{1}{2}\,\mathrm{erfc}\left(\frac{\ln\left(\frac{\pi r^3}{6\tilde{V}}\right) - \sigma_V^2}{\sqrt{2}\sigma_V}\right) - \sqrt[3]{\frac{9\pi}{128\tilde{V}}}\exp\left(-\frac{5\sigma_V^2}{18}\right)\mathrm{erfc}\left(\frac{3\ln\left(\frac{\pi r^3}{6\tilde{V}}\right) - 2\sigma_V^2}{3\sqrt{2}\sigma_V}\right) r \\ &+ \frac{\pi}{24\tilde{V}}\exp\left(-\frac{\sigma_V^2}{2}\right)\mathrm{erfc}\left(\frac{\ln\left(\frac{\pi r^3}{6\tilde{V}}\right)}{\sqrt{2}\sigma_V}\right) r^3.\end{aligned} \tag{7}$$

2.4 Attenuation model

In this study, we use the classical Weaver's attenuation model [12]. For statistically isotropic (untextured) polycrystals with equiaxed grains and using the Born approximation, the attenuation coefficient of the mode $I \in \{P,S\}$ propagating along the $\hat{\mathbf{p}}$ direction reads:

$$\alpha_I(\hat{\mathbf{p}}) = \frac{\pi\omega^4}{(4\delta_{IP}+8\delta_{IS})\rho^2 V_{0I}^3} \sum_J \frac{1}{V_{0J}^5} \int_{\mathcal{S}^2} Q_{I\to J}(\hat{\mathbf{p}}\cdot\hat{\mathbf{s}})\,\tilde{\eta}\left(\left|\frac{\omega}{V_{0I}}\hat{\mathbf{p}} - \frac{\omega}{V_{0J}}\hat{\mathbf{s}}\right|\right) \mathrm{d}\hat{\mathbf{s}}, \tag{8}$$

in which the integral is carried out over the unit sphere $\mathcal{S}^2$, δ_{ij} is the Kronecker delta, ω specifies the frequency of the wave, ρ denotes the constant density of the material, V_{0N} describes the background propagation velocity of the mode $N \in \{\mathrm{P},\mathrm{S}\}$, and $\tilde{\eta}$ is the Fourier transform of the TPCF, which is also known as the power spectral density function. Moreover, the function $Q_{I\to J}$ is the inner product of the covariance tensor which depends on the elastic tensor of single crystals and the propagation and polarization directions of incident and scattered waves [12].

In the low-frequency (Rayleigh) regime, the attenuation coefficients are proportional to $\omega^4 V_{\mathrm{eff}}$, where $V_{\mathrm{eff}} = \int \eta(r)\mathrm{d}\mathbf{r}$ is the effective grain volume. The three models predict starkly different dependencies for V_{eff} on the GSD width δ_D:

$$V_{\mathrm{eff}}^{\mathrm{AT}} = \pi\bar{D}^3(1+\delta_D^2)^3, \quad V_{\mathrm{eff}}^{\mathrm{Sha}} = \frac{\pi}{6}\bar{D}^3(1+\delta_D^2)^3, \quad V_{\mathrm{eff}}^{\mathrm{SK}} = \frac{\pi}{6}\bar{D}^3(1+\delta_D^2)^{12}. \tag{9}$$

Our model (SK) predicts a much more dramatic increase in effective volume and thus low-frequency attenuation, as the GSD width increases, scaling with $(1+\delta_D^2)^{12}$ compared to $(1+\delta_D^2)^3$ for the other models (AT and Sha).

3 Comparison of the proposed TPCF models

In this section, we first compare the analytical TPCF models and attenuation coefficients obtained via different models for polycrystals with an infinite number of grains. We then compare the TPCF and attenuation coefficients reported in a recent study [5] with those obtained using different correlation models.

3.1 Comparison for unbounded polycrystals

Figure 1 illustrates the TPCFs obtained for ten different grain size distribution widths δ_D in the interval $[0,1]$. The extreme cases are highlighted by the blue curve for $\delta_D = 0$ and the red curve for $\delta_D = 1$. Clear differences emerge among the models when grain size variability is introduced. For narrow distributions ($\delta_D \to 0$), the predictions from our formulation are nearly identical to those from Sha's model (Eq. (5)), while Argüelles and Turner's expression (Eq. (2)) produces substantially larger correlation lengths. On the other hand, when the distribution becomes broad as δ_D gets closer to 1, our model provides the longest correlation lengths, with Argüelles and Turner giving slightly lower values, and Sha's model showing the most rapid decay of the TPCF.

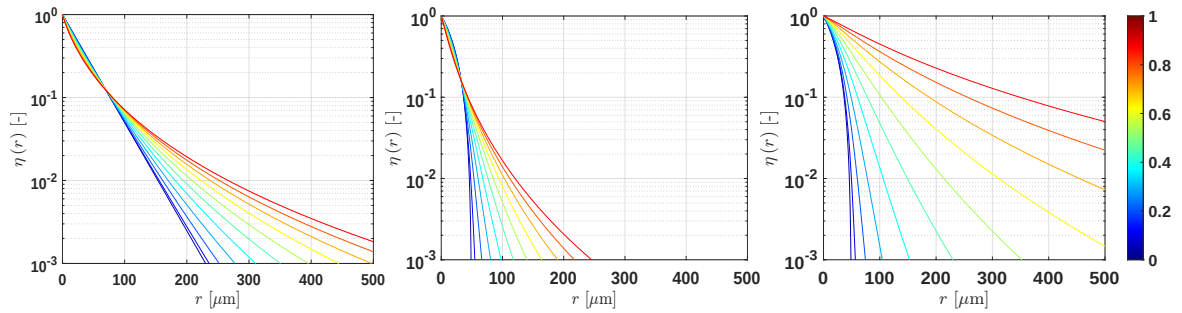

(a) AT (b) Sha (c) SK

Figure 1: TPCFs of microstructures with $\bar{D} = 50\,\mu$m and $\delta_D \in [0,1]$ based on different correlation models. Each curve corresponds to a δ_D value indicated by the colorbar.

Figure 2 depicts the variation of the normalized attenuation coefficient of P waves, $\alpha_P \bar{D}$, in terms of the normalized spatial frequency, $k_P \bar{D}$, for aluminum polycrystals. The single crystal elastic constants and density are $(c_{11}, c_{12}, c_{44}) = (103.4, 57.1, 28.6)$ GPa, and $\rho = 2700$ kg/m^3, respectively. For all correlation models, a broader grain size distribution leads to higher attenuations in the Rayleigh regime. Yet, their predictions diverge depending on the value of δ_D. When the distribution is narrow ($\delta_D \to 0$), our model closely matches Sha's, as both rely on the same limiting TPCF, while the Argüelles and Turner's model clearly overestimates attenuation. For moderate widths (*e.g.*, $\delta_D \approx 0.5$), our model becomes closer to the Argüelles and Turner prediction, whereas Sha's remains significantly lower. For broad distributions ($\delta_D \to 1$), our model produces the largest attenuation values, followed by Argüelles and Turner, with Sha's model giving the lowest values. These trends directly reflect the evolution of the associated TPCFs with δ_D.

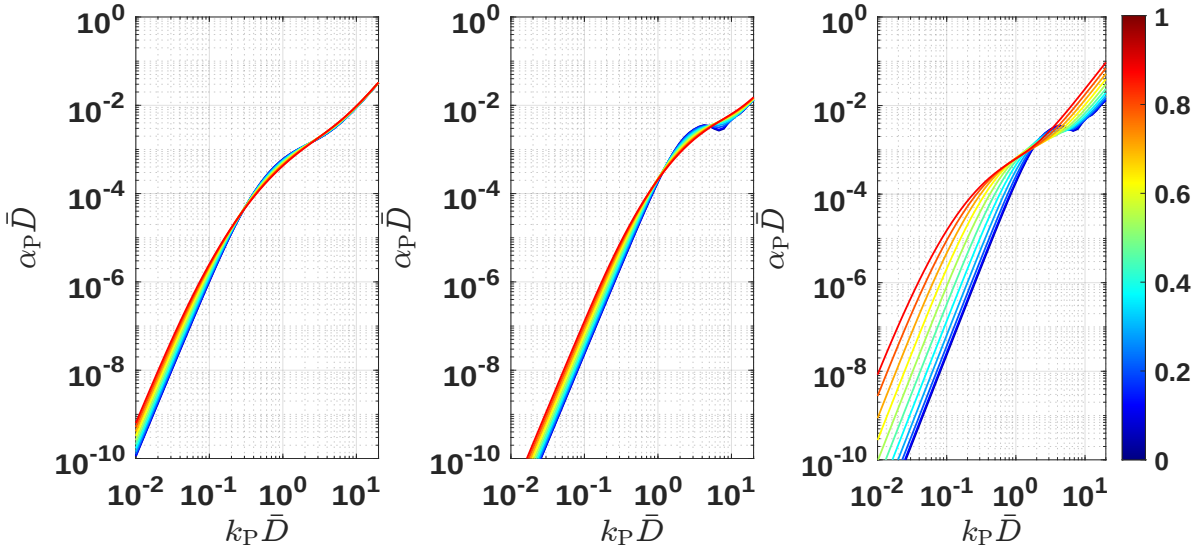

(a) AT (b) Sha (c) SK

Figure 2: Normalized P-wave attenuation coefficients for aluminum polycrystals with δ_D values in $[0, 1]$, computed using three TPCFs. Each curve corresponds to a δ_D value indicated by the colorbar.

Figure 2 also shows that in the Rayleigh regime, the usual fourth-order frequency dependence of attenuation, which holds for polycrystals with a single characteristic length scale, no longer applies when the grain size distribution is broad. Our model captures this breakdown at large δ_D, in agreement with numerical observations from [1] and experimental evidence from [2].

3.2 Comparison for synthetic polycrystals

In this section, the attenuation results obtained with the aforementioned TPCF models are compared against data recently reported by Islam and Turner [5] where they examined the effect of the grain size distribution width on ultrasonic attenuation using synthetic polycrystals previously generated in [3]. Their calculations rely on a modified version of Weaver's theory proposed in [4], which accounts for the finite size of the samples. In their approach, the form of the covariance function is not prescribed *a priori*.

The attenuation curves as functions of frequency were obtained for nickel polycrystals characterized by various grain size distribution widths, as illustrated in Fig. 6 of [5]. The relevant elastic constants and grain size statistics for the selected aggregates are listed in Table 1. Three representative microstructures were selected for comparison, all having an average grain size close to 30 μm and grain size distribution widths δ_D equal to 0.115, 0.433, and 0.633. The single crystal elastic constants and density are $(c_{11}, c_{12}, c_{44}) = (247, 153, 122)$ GPa, and $\rho = 8900$ kg/m^3, respectively.

We first focus on the TPCFs predicted by different correlation models described in Section 2, compared against the results reported in Fig. 5e of [5]. Figure 3 displays the numerical estimates obtained from thirty microstructural realizations (blue symbols), together with the analytical predictions from

Table 1: Grain size distribution parameters and grain numbers, taken from [5].

Set	$\bar{D}$ [μm]	δ_D [-]	N_g [-]
1	29.8	0.115	118130 ± 110
2	30.9	0.433	65812 ± 283
3	30.5	0.633	41444 ± 863

Argüelles and Turner (magenta dotted line), Sha (red dash-dot line), and the present model (black dashed line). For narrow grain size distributions (Fig. 3 (a)), both Sha's model and ours agree very well with the reference data, while the Argüelles and Turner model overestimates the TPCF. With increasing δ_D (Figure 3 (b) and (c)), the differences become more noticeable. Our formulation remains consistent with the reference curve across all cases, whereas the other two models are unable to reproduce the observed decay.

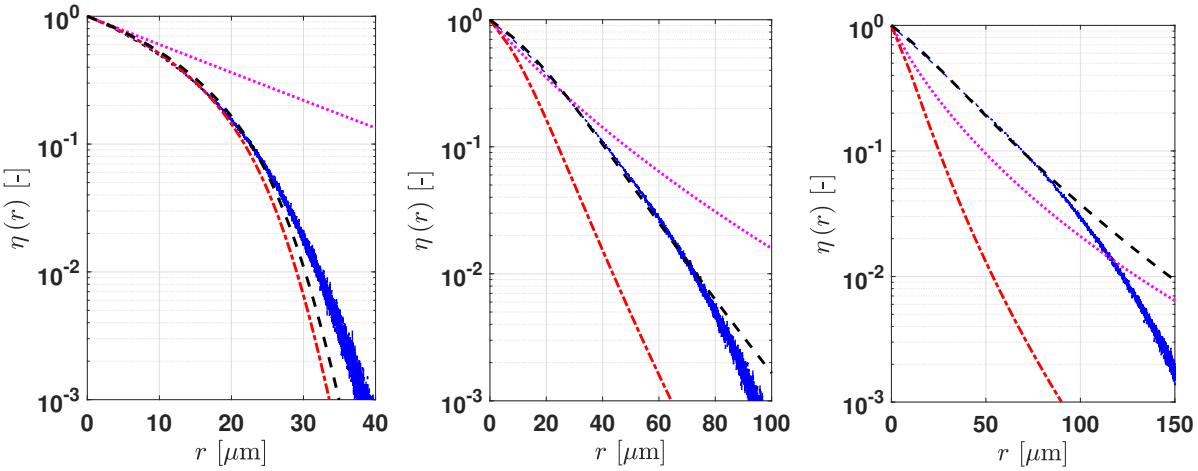

(a) $\delta_D = 0.115$ (b) $\delta_D = 0.433$ (c) $\delta_D = 0.633$

Figure 3: TPCFs predicted by the models of Argüelles and Turner (magenta dotted), Sha (red dash-dot), and Sheng and Khazaie (black dashed), compared with reported values from [5] (blue markers) for different values of δ_D.

Figure 4 compares the longitudinal attenuation predicted by all correlation models with the reference results presented in Fig. 6a of [5]. Because the vertical axis uses a logarithmic scale, the uncertainty bounds in the reference data are less noticeable here than in the original figure. For the smallest grain size distribution width considered (Figure 4(a)), both Sha's model and our formulation closely match the reported attenuation values, while the Argüelles and Turner model significantly overpredicts them, mainly due to its larger estimated correlation length. For the two broader distributions (Figure 4 (b) and (c)), our model is the only one that correctly follows the attenuation behavior documented in [5].

4 Conclusions

This work introduces a new closed-form spatial TPCF model that explicitly incorporates the volumetric grain size distribution through an analytical convolution based on spherical grain statistics, characterized by the mean grain diameter $\bar{D}$ and its coefficient of variation δ_D. When tested against numerical TPCFs extracted from numerous synthetic polycrystalline microstructures covering a broad range of distribution widths, the proposed formulation provides a closer match to the reference data than the models of Argüelles and Turner [1] and Sha [6]. The latter models cannot properly describe large grain size dispersions and lead to significant over- or underestimation of the spatial correlation. Coupling our TPCF with Weaver's theoretical framework then allowed us to evaluate the ultrasonic attenuation coefficient. The results reveal that the grain size distribution strongly influences attenuation in both the Rayleigh and stochastic regimes. Moreover, comparisons with available numerical attenuation data for some poly-

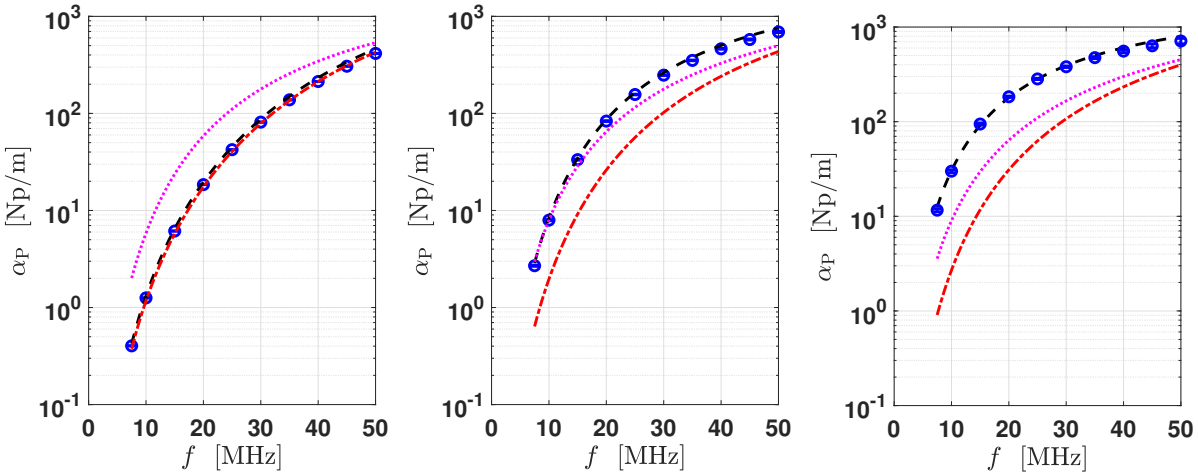

(a) $\delta_D = 0.115$ (b) $\delta_D = 0.433$ (c) $\delta_D = 0.633$

Figure 4: Longitudinal attenuation in terms of frequency predicted by the models of Argüelles and Turner (magenta dotted), Sha (red dash-dot), and our model (black dashed), compared with the values reported in [5] (blue markers) for different values of δ_D.

crystalline materials confirm the improved predictive capability of our approach, while the other models exhibit clear discrepancies.

References

[1] A.P. Argüelles, J.A. Turner. *Ultrasonic attenuation of polycrystalline materials with a distribution of grain sizes*, The Journal of the Acoustical Society of America, 141(6), 4347-4353, 2017.

[2] X. Bai, Y. Zhao, J. Ma, Y. Liu, Q. Wang. *Grain-size distribution effects on the attenuation of laser-generated ultrasound in α-titanium alloy*, Materials, 12(1), 102, 2018.

[3] M. Norouzian, S. Islam, J.A. Turner. *Influence of microstructural grain-size distribution on ultrasonic scattering*, Ultrasonics, 102, 106032, 2020.

[4] M. Norouzian, J.A. Turner. *Ultrasonic wave propagation predictions for polycrystalline materials using three-dimensional synthetic microstructures: Attenuation*, The Journal of the Acoustical Society of America, 145(4), 2181-2191, 2019.

[5] S. Islam, J.A. Turner. *Dataset for Quantifying the Effect of Ultrasonic Scattering from a Distribution of Grain Sizes*, Integrating Materials and Manufacturing Innovation, 1-9, 2025.

[6] G. Sha. *Correlation of elastic wave attenuation and scattering with volumetric grain size distribution for polycrystals of statistically equiaxed grains*, Wave Motion, 83, 102-110, 2018.

[7] N. Sheng, S. Khazaie. *A new correlation model for ultrasonic attenuation in polycrystals with broad grain size distributions*, Ultrasonics, 160, 107924, 2026.

[8] N. Sheng, S. Khazaie, M. Chevreuil, S. Fréour. *Influence of grain size distribution type on statistical moments of ultrasonic attenuations and phase velocities in random polycrystals*, Ultrasonics, 107800, 2025.

[9] N. Sheng, S. Khazaie, M. Chevreuil, S. Fréour. *On the statistical behavior of homogenized properties and ultrasonic phase velocities in random polycrystals*, International Journal of Solids and Structures, 285, 112531, 2023.

[10] F. E. Stanke, G. S. Kino. *A unified theory for elastic wave propagation in polycrystalline materials*, The Journal of the Acoustical Society of America, 75(3), 665-681, 1984.

[11] F. E. Stanke. *Spatial autocorrelation functions for calculations of effective propagation constants in polycrystalline materials*, The Journal of the Acoustical Society of America, 80(5), 1479-1485, 1986.

[12] R. L. Weaver. *Diffusivity of ultrasound in polycrystals*, Journal of the Mechanics and Physics of Solids, 38(1), 55-86, 1990.